Water Research, Volume 176, June 2020, Article number 115754
DOI:10.1016/j.watres.2020.115754

Establishing the mechanisms underpinning solids breakthrough in UASB configured anaerobic membrane bioreactors to mitigate fouling

K. M. Wang[a,b], A. Soares[b], B. Jefferson[b], H. Y. Wang[a], L. J. Zhang[c], S. F. Jiang[c], E. J. McAdam[b*]

[a] College of Environment, Zhejiang University of Technology, Hangzhou, 310014, China

[b] Cranfield Water Science Institute, Vincent Building, Cranfield University, Bedfordshire, MK43 0AL, UK

[c] College of Civil Engineering and Architecture, Zhejiang University of Technology, Hangzhou, 310014, China

*Corresponding author: e.mcadam@cranfield.ac.uk

Abstract

In this study, the mechanisms for solids breakthrough in upflow anaerobic sludge blanket (UASB) configured anaerobic membrane bioreactors (AnMBRs) have been described to establish design parameters for limiting membrane fouling. As the sludge blanket develops, two periods can be identified: (i) an initial progressive enhancement in solids separation provided through sludge blanket clarification, via depth filtration, which sustains downstream membrane permeability; and (ii) sludge blanket destabilisation, which imposed solids breakthrough resulting in a loss in membrane permeability. The onset of sludge blanket destabilisation was identified earlier in the flocculent AnMBR, which was ascribed to an increased gas production, caused by hydrolysis within the sludge blanket at extended solids residence time. Whilst hydrolysis also induced higher gas productivity within the granular AnMBR, solids breakthrough was not evidently observed during this period, and was instead only observed as the sludge blanket approached the UASB overflow. However, solids breakthrough was observed earlier for both reactors when treating wastewater with lower temperatures. This was explained through characterisation of the settling velocity of discrete particles from the sludge blanket of both MBRs; solids washout was evidenced to be induced by the increase in fluid viscosity with a reduction in temperature, which lowered terminal particle settling velocity. Nevertheless, particle settling velocity was comparable for particles from both sludge blankets. We therefore propose that the enhanced stability imparted by the granular AnMBR is due to the higher inertial force of the dense granular sludge. From this study, we suggest similarly low levels of membrane fouling can be achieved within flocculent AnMBR by managing solids retention time to constrain sludge bed height and excess

hydrolysis, together with adopting an upflow velocity based on particle buoyancy at the lowest expected operating temperature.

Keywords: *sewage; solids washout; upflow velocity; domestic wastewater; anaerobic MBR; fouling*

1. Introduction

Anaerobic processes for mainstream municipal wastewater treatment have gained increasing attention due to their advantage over conventional aerobic processes such as energy saving, biogas recovery and lower sludge production (Martin Garcia et al., 2013). Anaerobic membrane bioreactor (AnMBR) overcomes the drawbacks of conventional anaerobic treatment processes, notably washout of slow growing biomass, through effective solid-liquid separation allowing complete biomass retention (Gouveia et al., 2015a; Robles et al., 2012a; Smith et al., 2013). Comparison of AnMBR in upflow anaerobic sludge blanket (UASB) and completely stirred tank reactor (CSTR) configurations, have demonstrated UASB configured AnMBR to be beneficial for membrane fouling control (Martin-Garcia et al., 2011; Martin Garcia et al., 2013). The authors suggested this was due to the low solids environment in the membrane tank which led to lower fouling owing to less severe fouling from cake layer formation (Liao et al., 2006; Ozgun et al., 2013).

In UASB reactors, solids (particulate matter) from the influent is generally proposed to be first removed by physical processes including settling, adsorption and entrapment in the sludge bed (Lettinga et al., 2001). However, the reduced hydrolysis rate of entrapped particulate matter at low temperatures can be considered as a rate-limiting step (Lettinga et al., 2001), which increases the likelihood for solids accumulation in the UASB reactor. Membrane integration and recirculation of the concentrate flow from membrane tank to UASB reactor could exacerbate solids accumulation due to the prevention of solids losses by the membrane (Gouveia et al., 2015b; Ozgun et al., 2015a). Unless process interventions are adopted, the accumulated solid phase (particulate organic fraction) will wash out from the UASB into the membrane stage, imposing a reduction in membrane permeability (Gonçalves

et al., 2019; Ozgun et al., 2015a), and may offset the advantages of UASB configured AnMBR versus CSTR configured AnMBR.

Granular biomass has been shown to possess superior settling characteristics (Owusu-Agyeman et al., 2019) which prevent biomass washout and afford higher specific methanogenic activity (Lim and Kim, 2014) compared with flocculent inoculum biomass. In principle, this provides improved organics removal, increased energy recovery and better solid-liquid separation in granular UASB (G-UASB) versus flocculent UASB (F-UASB) reactors. However, granules do not actively grow in municipal wastewater, which introduces a cost of between 500 and 1000 USD per ton wet weight for procurement (Liu et al., 2002). There are few studies that directly compared granular and flocculent inoculum biomass within UASB and fewer studies that have applied granular biomass as inoculum in AnMBRs (Chu et al., 2005; Garcia et al., 2013; Gouveia et al., 2015a; Wang et al., 2019). Where comparisons have been made, feedwaters either comprised industrial or synthetic municipal wastewater, without a particulate organic fraction (Sabry, 2008; van Lier et al., 2015) which is considerably less of a challenge than posed with real municipal wastewater. Our previous study compared the membrane fouling of G-UASB and F-UASB configured AnMBR for municipal wastewater treatment and indicated that significantly higher membrane fouling was observed in the F-AnMBR at a lower temperature due to easier solids washout (Wang et al., 2019). However, the mechanism for solids accumulation and solids breakthrough have not been well understood in UASB and UASB configured AnMBR, and are critical to mitigate membrane fouling. In granular UASB, solids entrapment within the granular phase has also been observed when treating crude municipal wastewater, since the upflow velocity (V_{up}) (0.5-0.6 m h^{-1}, Uemura and Harada, 2000) was insufficient to expand the granular bed. Solids accumulation within the granular bed can lead to the washout of active biomass (Syutsubo et al., 2011), which will increase cost and result in the deterioration of methanogenic activity. Lester et al. (2013) demonstrated that by using an external recycle to increase V_{up} (1.0 m h^{-1}), sufficient granular fluidisation could be achieved to avoid solids accumulation and instead promote a stratified solids layer above the granular interface. Whilst not well studied, this dense solids layer may also promote solid-liquid separation, therefore improving the granular UASB treatment performance and the downstream membrane operation compared to that of flocculent UASB configured AnMBR (Lester et al., 2013).

Previous studies have characterised the accumulated solids within the sludge blanket along the height of the UASB, with a specific focus on solids concentration, particle size, microbial diversity, specific methanogenic activity, biodegradability and dewaterability (Gonçalves et al., 2019; Ozgun et al., 2019). However, the novelty of this study is in seeking to understand the impact of solids accumulation on UASB solid-liquid separation, thus establishing the mechanisms responsible for solids breakthrough, which can be used to inform the engineered design of UASB configured AnMBR. This is crucial to managing and sustaining membrane permeability in UASB configured AnMBRs, which presently offer the best opportunity to reduce membrane capital cost and energy demand for the anaerobic treatment of settled municipal wastewater. The specific objectives were therefore: (i) to investigate the impact of solids breakthrough in granular and flocculent UASB on the downstream membrane permeability; (ii) to evaluate the impact of the solids accumulation and sludge blanket formation on solids clarification for the downstream membrane; (iii) to evaluate the impact of solids retention and gas production on sludge blanket stability; and to (iv) investigate the impact of temperature on granular and flocculent UASB sludge blanket stability, reactor treatment performance, particle settling characteristics and membrane permeability.

2. Materials and methods

2.1 Anaerobic MBR pilot plant

Two 70 L cylindrical UASB reactors (0.2 m diameter x 1.8 m height) were operated in parallel (Model products, Wootton, UK) with a solid/liquid/gas separation (0.4 m diameter x 0.2 m height) at the top of the column, resulting in the effluent locating at about 2.0 m of the reactor (Figure 1). Three lamella settlers were utilised and the lowest separator reached at a column height of 1.5 m. The UASB columns had a total of five sampling points placed every 30 cm (Figure 1). The G-UASB was inoculated with 15 L of granular sludge (75% volatile solids (VS)) from a mesophilic UASB used for pulp and paper industry and F-UASB was seeded with 15 L flocculent sludge from an anaerobic digester treating a mixture of municipal primary and secondary sludges with 3.6% total solids (78% VS). Settled wastewater from Cranfield University's sewage treatment works was used as the feed, comprising total chemical oxygen

demand (COD_t), particulate COD (pCOD) and total suspended solids (TSS) of 244±92mg L^{-1}, 194±76mg L^{-1} and 129±38mg L^{-1} respectively was fed via the bottom of the two UASB reactors by peristaltic pump (520U, Watson Marlow, Falmouth, UK). Both G-UASB and F-UASB were operated at a hydraulic retention time (HRT) of 8 h for 360 days to acclimatise reactors before experimentation which was determined by the consistent removal of COD, biological oxygen demand (BOD_5), and the stabilisation of biogas production. An internal recycle was introduced by peristaltic pump (620S, Watson Marlow, Falmouth, UK) to sustain the V_{up} of 0.8-0.9 m h^{-1} (Tchobanoglous et al., 2003). The mixed gas and liquid velocity (V_{mix}) can be calculated as follows (Massey and Ward-Smith, 2006; Verberk et al., 2001):

$$V_{mix} = \frac{\dot{m}}{\rho_{mix} \cdot A} \quad (1)$$

$$\dot{m} = \rho_g Q_g + \rho_l Q_l \quad (2)$$

$$\rho_{mix} = \frac{\rho_g Q_g + \rho_l Q_l}{Q_g + Q_l} \quad (3)$$

where $\dot{m}$ is mass flow rate (kg s^{-1}), ρ_{mix} is the mixed fluid density (kg m^{-3}), A is the reactor cross-sectional area (m^2), ρ_g is the gas density (kg m^{-3}), ρ_l is the liquid density (kg m^{-3}), Q_g is the gas flow rate (m^3 s^{-1}), Q_l is the liquid flow rate (m^3 s^{-1}). Whilst averaged gas flow rates are commonly reported (c. 5 L CH_4 d^{-1}), peak gas flow rates of around 13 L h^{-1} are commonly recognised for short intervals due to the aggregation of produced methane into coarse bubbles, that impose an increased shear stress due to their higher rise rate (Lester et al., 2013).

The effluent from the granular and flocculent UASB overflowed into 30 L cylindrical membrane tanks (0.17 m diameter x 1.25 m height) to form a granular and flocculent AnMBR. The retentate with low dissolved oxygen (DO <0.2 mg L^{-1}) recycled from the membrane tank to the bottom of the UASB to sustain the upflow velocity. The membrane module (ZW-10) (SUEZ Water & Process Technologies, Oakville, Canada) consisted of four elements each of which comprised 76 polyvinylidene fluoride (PVDF) hollow fibres (0.52 m in length and 1.9 mm out diameter). The membrane has a nominal pore size of 0.04 µm, providing a total surface area of 0.93 m^2. Permeate was extracted at a net flux of 7.5 L m^{-2} h^{-1} by a peristaltic pump (520U, Watson Marlow, Falmouth, UK) for 10 mins followed by 1 min relaxation. The transmembrane pressure (TMP) was monitored by a pressure transducer (-1-1 bar, Gens sensor, Basingstoke, UK) in the permeate line recording by a data logger (ADC-2006, Pico Technology, St Neots, UK). Nitrogen-enriched air produced by a nitrogen generator (NG6,

Noblegen gas generator, Dunston, UK) was used for intermittent gas sparging (10s on/10s off) with a specific gas demand per membrane surface area (SGD_m) of 1.12 m^3 m^{-2} h^{-1}. Water flux was normalised to 20°C (Judd, 2011).

$$J_T = J_{20} \cdot 1.025^{(T-20)} \quad (4)$$

where J_T is the permeate flux at T °C, J_{20} is the permeate flux normalised to 20 °C, T is the temperature (°C). Following 200 h of operation (equivalent to a total filtered volume of 1500 L), total resistance was determined (R_t). The membrane resistance experiment was conducted in triplicate.

$$R_t = \frac{TMP}{\mu \cdot J} \quad (5)$$

The membrane was rinsed with tap water followed by chemical clean with 500 mg L^{-1} sodium hypochlorite overnight. Clean water permeability tests were conducted to ensure the membrane recovery before use. In order to evaluate the impact of temperature on system resilience, granular AnMBR and flocculent AnMBR were operated in both summer (phase I) and winter (phase II) periods with average sewage temperatures of 19.5±2.1 and 10.2±1.5 °C for 120 days and 60 days respectively (Table 1). The shorter operational time in the winter was due to the shorter time to achieve sludge blanket instability in the UASB reactor.

In the G-UASB, the granular sludge bed expanded to about 30% of the total column height and the light sludge fraction formed a sludge blanket layer above the granular sludge bed, which was constituted of dispersed growth flocs from the influent (Aiyuk et al., 2006; Chong et al., 2012). The sludge blanket height in the G-UASB was therefore measured as the total height of sludge blanket and inoculum granular matrix. Whilst for the F-UASB, there is no obvious differentiation between accumulated solids and inoculum flocculent sludge bed. The sludge blanket is presumed to function as a sludge blanket clarifier whose filtration performance can be determined as follows:

$$\text{pCOD } (C/C_0) = \frac{\text{UASB effluent pCOD concentration}}{\text{UASB influent pCOD concentration}} \quad (6)$$

A regressive technique (Chow test) was applied to determine whether the transition between stable and unstable periods is better described by multiple regressions or a pooled regression. Data was divided into two subgroups: stable and unstable periods, and the sum of the square residuals (SSR) between predicted and experimental data calculated. The sum of SSR for each

period was calculated and the minimum determined statistically which evidenced the transition between stable and unstable periods of operation. To validate the statistical validity of the identified transition between regions, the F test was subsequently applied:

$$F = \frac{(SSR_p - SSR_1 - SSR_2)/2}{(SSR_1 + SSR_2)/(N-4)} \quad (7)$$

where SSRp, SSR1 and SSR2 are SSR of pooled regression, first group and second group respectively, N is number of data points. The light flocculent sludge blanket in the G-UASB and flocculent sludge bed in the F-UASB were withdrawn once solids washout into the UASB effluent was noted by an increase of suspended solids concentration and reset to their initial height. No obvious loss in granules was observed, as evidenced by the sustained granule bed height. Therefore, the primary seeded material (granular and flocculent) was resident for the full period, i.e. during start-up, operation and through to completion of the experiments. The SRT of the secondary material, which accumulates above the seeded active biomass emanating from flocculated material within the feed, was about 120 days and 60 days in phase I and phase II, respectively (Table 1).

Sludge particle settling velocities (flocculent sludge collected from above the granule bed in the G-UASB and flocculent sludge in the F-UASB) were tested in a temperature-controlled water bath at 10 and 20 °C to establish whether floc properties could explain solids breakthrough. Based on the data at a water temperature of 10 °C, particle settling velocities at a water temperature of 20 °C were predicted by applying Stoke's law (particle Reynolds number <1.0) (Tchobanoglous et al., 2003):

$$v_p = \frac{g(\rho_p - \rho_w)d_p^2}{18\mu} \quad (8)$$

where V_p is particle settling velocity (m s^{-1}), ρ_p is particle density (kg m^{-3}), ρ_w is liquid density (kg m^{-3}), d_p is particle diameter (m), μ is the liquid viscosity (Pa. s). The confidence interval of 95 % for prediction values were calculated. Settling column apparatus consisted of a central settling column containing deionised water enclosed by a water bath to control the temperature at 10 or 20 °C. The sludge particles were introduced into a settling column via a taped entry port with a wide-mouthed pipette to ensure the particles settle in the centre of the column. Particle images were captured by a Sony ICX674 sensor (Infinity 3-3UR, Lumenera Corporation, Ottawa, Canada). An image analysis software (Image-Pro Premier 9) was used to analyse the particle size and settling velocity. All analysis was conducted in triplicate.

2.2 Analytical methods

Suspended solids (SS) and BOD_5 were measured according to standard methods (APHA, 2005). Total and soluble chemical oxygen demand (COD) were analysed with Merck test kits (Merck KGaA, Darmstadt, Germany). Soluble COD (sCOD) was measured after filtering with 1.2 µm filter paper (70 mm Glass Fibre Filter Paper Grade GF/C, Whatman, GE Healthcare Life Sciences, Little Chalfont, UK). Particle size was measured by a laser diffraction particle size analyser (Mastersizer 3000, Malvern Instruments Ltd, Malvern, UK). Biogas flow rate was measured with a gas meter (TG0.5, Ritter, Bochum, Germany). Methane (CH_4) composition was analysed by a gas analyser (Servomex 1440, Crowborough, UK). Sludge blanket height was observed and measured daily.

The data sets were first analysed for normal distribution through Shapiro-Wilk tests to determine the application of parametric and non-parametric statistical tools. Parametric data were examined with ANOVA tests whilst non-parametric data were examined with Mann-Whitney U test for independent data. All the statistically significant differences were based on 95 % of the confidence level ($p<0.05$).

3. Results and discussion

3.1 *Solids breakthrough reduces membrane permeability*

The bulk sludge characterisation within the membrane tank typically comprised pCOD of around 220-250 mg L^{-1}. However, following a long period of sludge blanket development at an average temperature of 20°C, the particulate fraction suddenly increased to between 460 and 520 mg pCOD L^{-1} for both granular and flocculent systems (Table 2). This can be accounted for a sudden destabilisation in the sludge blanket, which might be due to the high sludge blanket height with limited empty space for particle energy dissipation and has been observed elsewhere (Ozgun et al., 2015a; Wang et al., 2019). The increase rate of membrane total resistance within 200 h operation also rose by 1.2-1.3 times for G-AnMBR and F-AnMBR (Figure 2). After 200 h operation, the total membrane resistance also increased by approximately 36% ($p<0.05$) and 80% ($p<0.05$) for G-AnMBR and F-AnMBR respectively (Figure 3). This was equivalent to a total membrane resistance of 4.2×10^{12} m^{-1} for F-AnMBR

which was around 1.2 times the membrane resistance encountered with G-AnMBR ($p<0.05$). When operated during a period of lower temperature (from 7.8 to 13.5°C), a greater increase of pCOD in the membrane tank was again observed with average concentration of 700-820 mg pCOD L^{-1}, representing an increase of 1.8 times compared to when operating at 19.5±2.1°C, and was more evident with the flocculent matrix (Table 2). Although SMP_{COD} increased at lower temperatures from 80-95 mg L^{-1} to 130-170 mg L^{-1} by 1.6-1.8 times (including during sludge blanket development) due to the higher SMP production at lower temperature (Ozgun et al., 2015b), SMP further increased 1.1-1.9 times when the sludge blanket became unstable (Table 2). This introduced 33% ($p<0.05$) and 64% ($p<0.05$) increase in total membrane resistance compared with that during the sludge blanket development period. The increase rate of membrane total resistance within 200 h operation also rose by 1.2 and 2.0 times for G-AnMBR and F-AnMBR respectively (Figure 2). In conventional aerobic MBR, which typically operate at solids concentration exceeding 10gMLSS L^{-1}, it has been observed that a further increase in solids concentration does not obviously influence membrane permeability (Judd, 2011). However, where lower solids concentrations have been studied through the reduction in solids retention time (SRT), an increase in membrane fouling is acknowledged due to the higher colloidal matter concentrations (Yoon, 2015). In AnMBR, the relationship between biomass and dissolved/colloidal matter is different, as SMP tends to accumulate with biomass or at high SRT (Robles et al., 2012b; Wang et al., 2018). Therefore low bulk sludge suspended solids may be conducive for membrane fouling control (Liao et al., 2006). Martin et al. (2013) compared membrane fouling propensity of a granular UASB configured AnMBR and flocculent CSTR configured AnMBR with MLSS of less than 0.6 and 7.7g L^{-1} and SMP_{COD} of 198 and 598 mg L^{-1} respectively. The authors suggested that lower membrane fouling propensity was obtained in the granular system with low solids and colloidal matter loading. The increase in membrane fouling observed following solids washout into the membrane tank associated to long term UASB operation (Figure 4) or from a reduction in fluid temperature (Table 2, Table 3), can therefore be accounted for by the increased solids loading onto the membrane. It is also suggested that exposure of this solids fraction to gas sparging within the membrane tank may have increased the colloidal fraction of the suspension, which has been well recognised to introduce more tenacious fouling (Lin et al., 2009; Martin-Garcia et al., 2011). This increase in colloidal material is supported by the significant increase of SMP_{COD} in the bulk sludge

especially during blanket destabilisation period at a lower average temperature for both granular and flocculent systems (Table 2).

3.2 Clarification introduced through sludge blanket formation reduces solids fraction downstream

The sludge blanket height was monitored in the granular and flocculent UASB configured AnMBR (Figure 4) and measured as a function of the total working height of the bed (set by the effluent discharge port, X/X_0) from 0.25 to 0.72-0.75. A regressive technique (Chow test) was applied to test whether there were two statistically distinct datasets formed for confirmation of the transition point between the sludge blanket development and blanket destabilisation period (Figure 4). During the sludge blanket development period, progressive sludge blanket height increase was observed until a 'steady-state' sludge blanket height was reached at around X/X_0 0.75, equivalent to the base of the three-phase separator. A sudden decrease in sludge blanket subsequently occurred with an apparent increase in effluent pCOD to around 186 mg L^{-1}. This leads to less than 5% pCOD removal compared with the average pCOD concentration of 194±76mg L^{-1} in the influent, which suggests the sludge blanket destabilisation and occurrence of pCOD breakthrough (Figure 5). This was coincident with the significant increase of pCOD and SMP_{COD} concentrations (Table 2) in the membrane tank and subsequently higher membrane fouling rate as discussed in Section 3.1 (Figure 2, Figure 3).

Characterisation of particle separation within the sludge blanket of the UASB demonstrated a progressive increase in solids separation from C/C_0 0.8 at the outset of treatment to C/C_0 of <0.20 after treating 9 m^3 wastewater, for both G-UASB and F-UASB configured AnMBRs (Figure 5). This improvement in particle separation following the increase in sludge blanket height is characteristic of depth filtration more commonly associated with sludge blanket clarifiers. The longer bed lengths, extend contact time and tortuosity for particles migrating through the bed, which increases the probability for collision and attachment within the developing sludge bed (Ives, 1968). During sludge blanket development, effluent particle sizes comprised bimodal distributions with peaks centred below 2 µm and between 111 and 127 µm for granular and flocculent UASB respectively (Figure 6). This compares favourably to the feed, which comprised a unimodal particle size

distribution centred around a larger fraction of coarse aggregated material, providing confirmatory evidence for the preferential segregation of coarse particles during filtration of the bed (Landa et al., 1997), and emphasises the critical role of sludge blanket development to the dissipation of solids loading downstream on the membrane, particularly important in AnMBR due to the increased rate of solids accumulation introduced by the membrane.

The physical separation mechanism described herein is supported by more qualitative data for high pCOD removal reported for low temperature municipal wastewater treatment (Lester et al., 2013; Uemura and Harada, 2000). However, following a period of sludge blanket development, the blanket destabilised as demonstrated through a loss in sludge blanket height (Figure 4), coupled with a breakthrough of pCOD into the effluent (Figure 5). Sludge blanket destabilisation was observed in F-UASB at around half of the hydraulic throughput of G-UASB. During this phase, the particle size of the effluent pCOD increased as illustrated by a further peak centred at 955 and 1445 µm for F-UASB and G-UASB respectively (Figure 6). Solids breakthrough has been similarly observed in several previous studies at high sludge bed height (Gonçalves et al., 2019). Progressive development of sludge blanket height leads to greater local solids consolidation within the bed and a more tortuous path for flow such that channelling occurs, which introduces elevated local velocities at the solid-liquid interface above the sludge blanket, as visually evidenced by local jetting effects (Lester et al., 2013). A minimum column length is subsequently demanded for particle energy dissipation upon release from the sludge bed. Sufficient empty bed length above the sludge blanket is therefore demanded to avoid the solids washout that leads to the membrane permeability decline.

3.3 Solids retention time and gas production introduce sludge destabilisation

A broadly linear increase in gas production was observed during sludge blanket development, while liquid phase temperatures were relatively stable. However, following 10-15 m^3 wastewater treated, or between 45 and 70 days operation, a peak in gas production of 6.7 and 8.1 L d^{-1} was observed for both G-UASB and F-UASB configured AnMBR with a methane content of 62-68%, which corresponded to a small increase in liquid temperature (18-24°C, Figure 6). This peak is coincident with the onset of blanket instability within the F-UASB, whilst the G-UASB was able to produce a further 10 m^3 wastewater before the sludge blanket

destabilised (Figure 5). Peak gas production can be attributed to the partial hydrolysis of the entrapped particulate matter (within the upper flocculated section) due to the extended SRT for this sludge fraction under relatively low temperatures. Hydrolysis is presumed rate limiting for methanogenesis, as it is first-order with respect to temperature (Lew et al., 2009). Lettinga et al. (2001) estimated that an SRT of 75 days was required to achieve sufficient hydrolysis at a lower liquid temperature of 15°C compared to 15 days at a liquid temperature of 25°C (Lettinga et al., 2001). This projected period for the onset of hydrolysis broadly corresponds to the time required for peak gas production and is supported by a significant increase in effluent sCOD concentration ($p<0.05$) during the period of peak gas production, which is suggestive of the conversion of entrapped particulate COD to sCOD (Figure S1) (Lew et al., 2004). Whilst averaged gas flow rates are reported (Figure 7), these comprise a cycle of peak gas flow rates of short duration (around 300 L d^{-1}, for only 30 seconds), which increases the local superficial upflow velocity from 222 µm s^{-1} to a combined velocity of 339 µm s^{-1} (Eq. 3). We suggest that it is this increase in superficial velocity which increased the probability for sludge destabilisation in F-UASB. The comparative stability of the G-UASB can be explained by the larger particle size and higher density of granular sludge (0.5-3 mm), compared to flocculent sludge (10 to 150 µm) which introduces greater inertia (Tsutsumi et al., 1999) and subsequently improves energy dissipation, thereby reducing mixing in the granular system. This was evidenced in this study by a more stable sludge blanket in the granular UASB configured AnMBR compared with flocculent UASB configured AnMBR. It is therefore suggested to keep the SRT below 45 days especially for the flocculent systems, in order to avoid the sludge blanket destabilisation due to the partial hydrolysis within the sludge blanket at extended solids residence time. However, this is an arbitrary value, which was strongly dependent on mixing conditions and solution temperature.

3.4 Increased fluid viscosity at a lower temperature increases solids breakthrough

The impact of temperature on sludge blanket stability was investigated in two periods corresponding to average sewage temperatures of 19.5±2.1 and 10.2±1.5°C (Figure 8). Breakthrough curves illustrate a marked increase in effluent pCOD concentration at a low average temperature of 10°C for both granular and flocculent systems. For example, the 75th percentiles for pCOD removal for the F-UASB were 78.3% and 55.1% at 19.5 and 10.2°C

respectively. For comparison, 75th percentiles for pCOD removal with G-UASB were 78.0% and 65.7% respectively, suggesting that pCOD removal in the G-UASB is more consistent at lower temperature. For this low temperature period, a significant difference (p<0.05) in average pCOD removal efficiency was observed between the F-UASB and G-UASB reactors corresponding to 45±22% and 52±18% respectively (Table 3).

Whilst previous literature has similarly noted washout from UASB treating municipal wastewater following a reduction in temperature (Lew et al., 2004; Syutsubo et al., 2011), the mechanism is not well described. Consequently, the impact of temperature on particle settling velocity was subsequently conducted in a temperature-controlled environment set to the temperatures encountered during treatment, and the flocculated sludge collected from the top of the G-UASB (the flocculent fraction) and F-UASB compared (Figure 9). When particles from the same system were compared at two temperatures, higher particle settling velocities were observed for the higher temperature water (Figure 9a,b). It is asserted that the reduction in settling velocity at lower temperature is therefore due to the increase in viscosity (Eq. 8). This is supported by the prediction of particle settling velocity at 20°C from data collected at 10 °C through transformation of Stoke's law (Figure 9a), which was fitted within 95 % confidence intervals. For illustration of the significance to operation of AnMBR at low temperature, particle settling data at 10°C intersects the line denoting the superficial velocity fixed by the liquid and when combined with gas production, which evidences the increased probability for sludge destabilisation and washout at lower temperatures, since the particle settling velocity is not sufficient to offset the settling velocity imposed. Since the sludge blanket of the G-AnMBR has been shown to provide more robust pCOD separation at lower temperatures, the two matrices were compared and the data shown to overlay each other (Figures 9c and d). Comparable particle settling behaviour for both matrices provides further supporting evidence that it is the inertia of the granular sludge beneath the flocculated layer within the G-AnMBR that extends the time to sludge blanket destabilisation. In G-AnMBR, a minimum upflow velocity of 0.8 m h^{-1} is required to ensure sufficient expansion to avoid clogging and enable the formation of the upper flocculated layer. Lew et al. (2004) instead proposed an upflow velocity of 0.35 m h^{-1} in order to limit solids washout during treatment of settled municipal wastewater at 10-28°C. As evidenced in this study through particle settling characterisation, this is sufficient to minimise solids washout at low sewage

temperatures (10°C) and could be adopted into F-UASB to improve robustness. It has been confirmed by significantly lower pCOD and SMP_{COD} concentrations in the membrane tank with upflow velocity of 0.35 m h^{-1} compared with that of 0.8 m h^{-1}, and could be sufficient to deliver similar separation behaviour to G-UASB (Wang et al., 2019).

4. Conclusions

This study evaluated the mechanisms underpinning solids breakthrough in both granular and flocculent UASB configured AnMBRs, in order to identify operating conditions that can minimise solids washout to sustain membrane permeability. During the sludge blanket development period, solids accumulation in the sludge blanket enhanced pCOD entrapment and sustained membrane permeability, which can be explained by the clarification introduced through the sludge blanket formed either within the F-UASB sludge bed or above the granular matrix in the G-UASB. However, sludge blanket destabilisation induced solids breakthrough significantly reducing membrane permeability. It is therefore suggested to control the sludge blanket at a threshold through solids withdrawl to ensure sufficient empty bed length above the sludge blanket, in order to improve energy dissipation of the solid phase to minimise solids washout and subsequently sustain the AnMBR membrane operation. The solids washout was exacerbated by higher biogas production for the flocculent system, which was introduced through partial hydrolysis of the entrapped particulate matter at an extended solids retention time (SRT). Therefore, controlling SRT within the sludge blanket to around 45 days should provide an optima between solids separation manifested by depth filtration and an excess biogas production especially for the flocculent systems, which promotes solids washout. A reduction in liquid temperature increased instability of the sludge blanket for both granular and flocculent matrices, introducing considerably membrane fouling. This can be explained by the reduced particle settling velocity that occurs due to the increase in wastewater viscosity at lower temperatures. The AnMBR seeded with granular biomass demonstrated better stability particularly at low temperatures; this would indicate sustaining a high upflow velocity for G-UASB which allows sufficient bed expansion to limit solids accumulation within the granules, whilst reducing upflow velocity for F-UASB to minimise solids washout. Such interventions will not only improve downstream membrane fouling but could also enable similar membrane permeabilities within flocculent UASB configured AnMBR

to those achieved with granular UASB configured AnMBR, which could lower the cost and associative risk of implementing AnMBR for sewage treatment.

Acknowledgements

The authors would like to thank the PhD project industrial sponsors Anglian Water, Scottish Water, Severn Trent Water and Thames Water. Dr. Wang is now working in Zhejiang University of Technology as a lecturer.

References

Aiyuk, S., Forrez, I., Lieven, D.K., van Haandel, A., Verstraete, W., 2006. Anaerobic and complementary treatment of domestic sewage in regions with hot climates-A review. Bioresour. Technol. 97, 2225–2241.

APHA, 2005. Standard Methods for the Examination of Water and Wastewater, 21st ed. American Public Health Association, Washington D.C.

Chong, S., Sen, T.K., Kayaalp, A., Ang, H.M., 2012. The performance enhancements of upflow anaerobic sludge blanket (UASB) reactors for domestic sludge treatment - A State-of-the-art review. Water Res. 46, 3434–3470.

Chu, L.B., Yang, F.L., Zhang, X.W., 2005. Anaerobic treatment of domestic wastewater in a membrane-coupled expended granular sludge bed (EGSB) reactor under moderate to low temperature. Process Biochem. 40, 1063–1070.

Garcia, I., Mokosch, M., Soares, A., Pidou, M., Jefferson, B., 2013. Impact on reactor configuration on the performance of anaerobic MBRs :treatment of settled sewage in temperate climates. Water Res. 47, 4853–4860.

Gonçalves, R.F., Louzada, L.M., Wanke, R., 2019. A sludge purging procedure that increases the robustness of upflow anaerobic sludge blanket reactors in sewage treatment. Int. J. Environ. Sci. Technol. 6, 7943–7952.

Gouveia, J., Plaza, F., Garralon, G., Fdz-Polanco, F., Peña, M., 2015a. A novel configuration for an anaerobic submerged membrane bioreactor (AnSMBR). Bioresour. Technol. 198, 510–519.

Gouveia, J., Plaza, F., Garralon, G., Fdz-Polanco, F., Peña, M., 2015b. Long-term operation of a pilot scale anaerobic membrane bioreactor (AnMBR) for the treatment of municipal wastewater under psychrophilic conditions. Bioresour. Technol. 185, 225–233.

Ives, K.J., 1968. Theory of operation of sludge blanket clarifiers. Proc. Inst. Civ. Eng. 39, 243–260.

Judd, S.J., 2011. Principles and Applications of Membrane Bioreactors in Water and Wastewater Treatment, 2nd ed. Elsevier, London,UK.

Landa, H., Capella, A., Jimenez, B., 1997. Particle size distribution in an efluent from an advanced primary treatment and its removal during filtration. Water Sci. Technol. 36, 159–165.

Lester, J., Jefferson, B., Eusebi, A.L., Mcadam, E., Cartmell, E., 2013. Anaerobic treatment of fortified municipal wastewater in temperate climates. J. Chem. Technol. Biotechnol. 88, 1280–1288.

Lettinga, G., Rebac, S., Zeeman, G., 2001. Challenge of psychrophilic anaerobic wastewater treatment. Trends Biotechnol. 19, 363–370.

Lew, B., Tarre, S., Belavski, M., Green, M., 2004. UASB reactor for domestic wastewater treatment at low temperatures: A comparison between a classical UASB and hybrid UASB-filter reactor. Water Sci. Technol. 49, 295–301.

Liao, B.Q., Kraemer, J.T., Bagley, D.M., 2006. Anaerobic membrane bioreactors: applications and research directions. Crit. Rev. Environ. Sci. Technol. 36, 489–530.

Lim, S.J., Kim, T., 2014. Applicability and trends of anaerobic granular sludge treatment processes. Biomass and Bioenergy 60, 189–202.

Lin, H.J., Xie, K., Mahendran, B., Bagley, D.M., Leung, K.T., Liss, S.N., Liao, B.Q., 2009. Sludge properties and their effects on membrane fouling in submerged anaerobic membrane bioreactors (SAnMBRs). Water Res. 43, 3827–3837.

Liu, Y., Xu, H.L., Show, K.Y., Tay, J.H., 2002. Anaerobic granulation technology for wastewater treatment. World J. Microbiol. Biotechnol. 18, 99–113.

Martin-Garcia, I., Monsalvo, V., Pidou, M., Le-Clech, P., Judd, S.J., McAdam, E.J., Jefferson, B., 2011. Impact of membrane configuration on fouling in anaerobic membrane bioreactors. J. Memb. Sci. 382, 41–49.

Martin Garcia, I., Mokosch, M., Soares, A., Pidou, M., Jefferson, B., 2013. Impact on reactor configuration on the performance of anaerobic MBRs: Treatment of settled sewage in temperate climates. Water Res. 47, 4853–4860.

Massey, B.S., Ward-Smith, A.J., 2006. Mechanics of Fluids, Eight. ed. Taylor & Francis, UK.

McAdam, E.J., Judd, S.J., 2008. Optimisation of dead-end filtration conditions for an immersed anoxic membrane bioreactor. J. Memb. Sci. 325, 940–946.

Owusu-Agyeman, I., Eyice, Ö., Cetecioglu, Z., Plaza, E., 2019. The study of structure of anaerobic granules and methane producing pathways of pilot-scale UASB reactors treating municipal wastewater under sub-mesophilic conditions. Bioresour. Technol. 290, 121733.

Ozgun, H., Dereli, R.K., Ersahin, M.E., Kinaci, C., Spanjers, H., van Lier, J.B., 2013. A review of anaerobic membrane bioreactors for municipal wastewater treatment: Integration options, limitations and expectations. Sep. Purif. Technol. 118, 89–104.

Ozgun, H., Ersahin, M.E., Zhou, Z., Tao, Y., Spanjers, H., van Lier, J.B., 2019. Comparative evaluation of the sludge characteristics along the height of upflow anaerobic sludge blanket coupled ultrafiltration systems. Biomass and Bioenergy 125, 114–122.

Ozgun, H., Gimenez, J.B., Evren, M., Tao, Y., Spanjers, H., van Lier, J.B., 2015a. Impact of membrane addition for effluent extraction on the performance and sludge characteristics of upflow anaerobic sludge blanket reactors treating municipal wastewater. J. Memb. Sci. 479, 95–104.

Ozgun, H., Tao, Y., Ersahin, M.E., Zhou, Z., Gimenez, J.B., Spanjers, H., van Lier, J.B., 2015b. Impact of temperature on feed-flow characteristics and filtration performance of an upflow anaerobic sludge blanket coupled ultrafiltration membrane treating municipal wastewater. Water Res. 83, 71–83.

Robles, A., Ruano, M.V., García-Usach, F., Ferrer, J., 2012a. Sub-critical filtration conditions of commercial hollow-fibre membranes in a submerged anaerobic MBR (HF-SAnMBR) system: the effect of gas sparging intensity. Bioresour. Technol. 114, 247–254.

Robles, A., Ruano, M.V., Ribes, J., Ferrer, J., 2012b. Sub-critical long-term operation of industrial scale hollow-fibre membranes in a submerged anaerobic MBR (HF-SAnMBR) system. Sep. Purif. Technol. 100, 88–96.

Sabry, T., 2008. Application of the UASB inoculated with flocculent and granular sludge in treating sewage at different hydraulic shock loads. Bioresour. Technol. 99, 4073–4077.

Smith, A.L., Skerlos, S.J., Raskin, L., 2013. Psychrophilic anaerobic membrane bioreactor treatment of domestic wastewater. Water Res. 47, 1655–1665.

Syutsubo, K., Yoochatchaval, W., Tsushima, I., Araki, N., Kubota, K., Onodera, T., Takahashi, M., Yamaguchi, T., Yoneyama, Y., 2011. Evaluation of sludge properties in a pilot-scale UASB reactor for sewage treatment in a temperate region. Water Sci. Technol. 64, 1959–1966.

Tchobanoglous, G., Burton, F.L., Stensel, H.D., 2003. Wastewater Engineering Treatment and Reuse, 4th ed. McGraw-Hill Companies, New York.

Tsutsumi, A., Chen, W., Kim, Y.H., 1999. Classification and characterization of hydrodynamic and transport behaviors of three-phase reactors. Korean J. Chem. Eng. 16, 709–720.

Uemura, S., Harada, H., 2000. Treatment of sewage by a UASB reactor under moderate to low temperature conditions. Bioresour. Technol. 72, 275–282.

van Lier, J.B., van der Zee, F.P., Frijters, C.T.M.J., Ersahin, M.E., 2015. Celebrating 40 years anaerobic sludge bed reactors for industrial wastewater treatment. Rev. Environ. Sci. Bio/Technology 14, 681–702.

Verberk, J.Q.J.C., Worm, G.I.M., Futselaar, H., van Dijk, J.C., 2001. Combined air-water flush in dead-end ultrafiltration. Water Sci. Technol. Water Supply 1, 393–402.

Wang, K.M., Martin Garcia, N., Soares, A., Jefferson, B., McAdam, E.J., 2018. Comparison of fouling between aerobic and anaerobic MBR treating municipal wastewater. H2Open J. 1, 131–159.

Wang, K.M., Soares, A., Jefferson, B., McAdam, E.J., 2019. Comparable membrane permeability can be achieved in granular and flocculent anaerobic membrane bioreactor for sewage treatment through better sludge blanket control. J. Water Process Eng. 28, 181–189.

Yoon, S.H., 2015. Membrane Bioreactor Processes: Principles and Applications. CRC press.

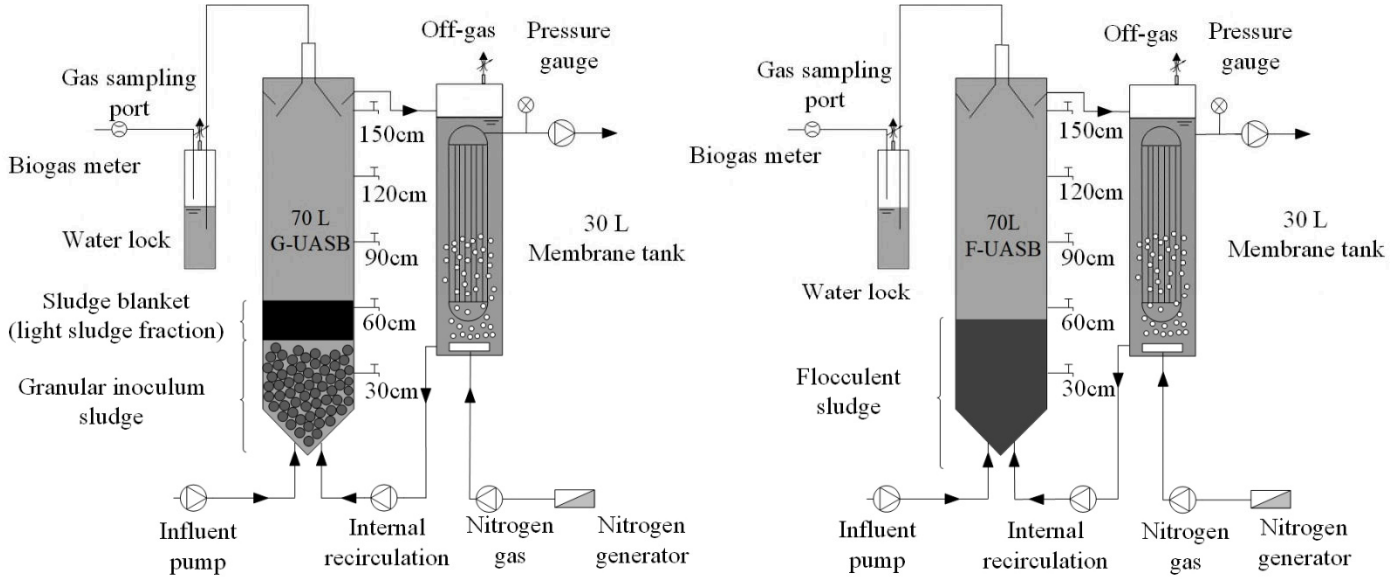

Figure 1. Schematics of the granular UASB configured AnMBR and flocculent UASB configured AnMBR.

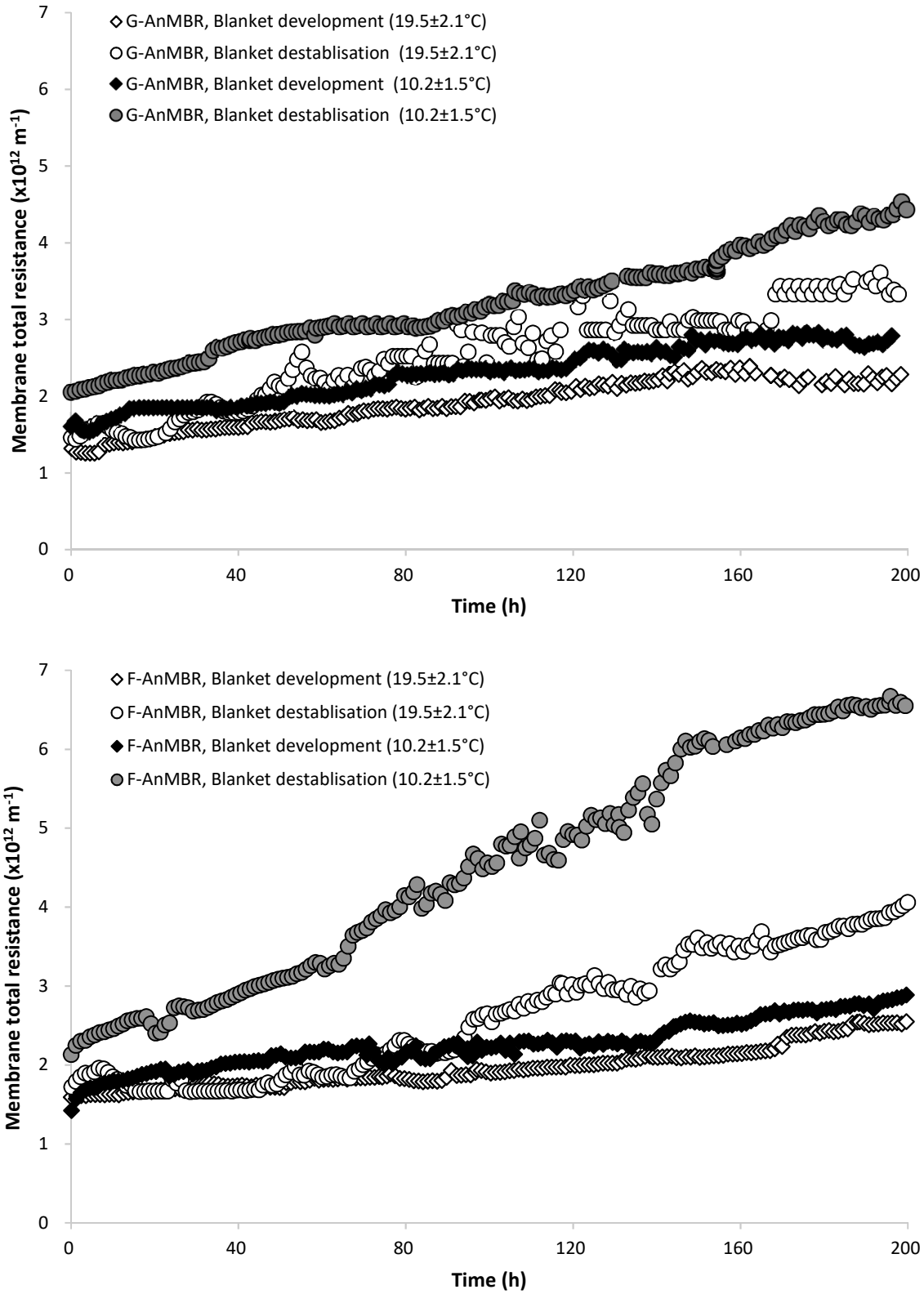

Figure 2. Temporal fouling trends (membrane total resistance) in granular and flocculent AnMBR during sludge blanket development and blanket destabilisation at an average temperature of 10 and 20°C. Filtration/relaxation, 10min on/1min off, $J_{20\,net}$, 7.5 L m^{-2} h^{-1}; gas sparging, 10s on/10s off, SGD_m, 1.12 m^3 m^{-2} h^{-1}. Flux normalised to 20°C.

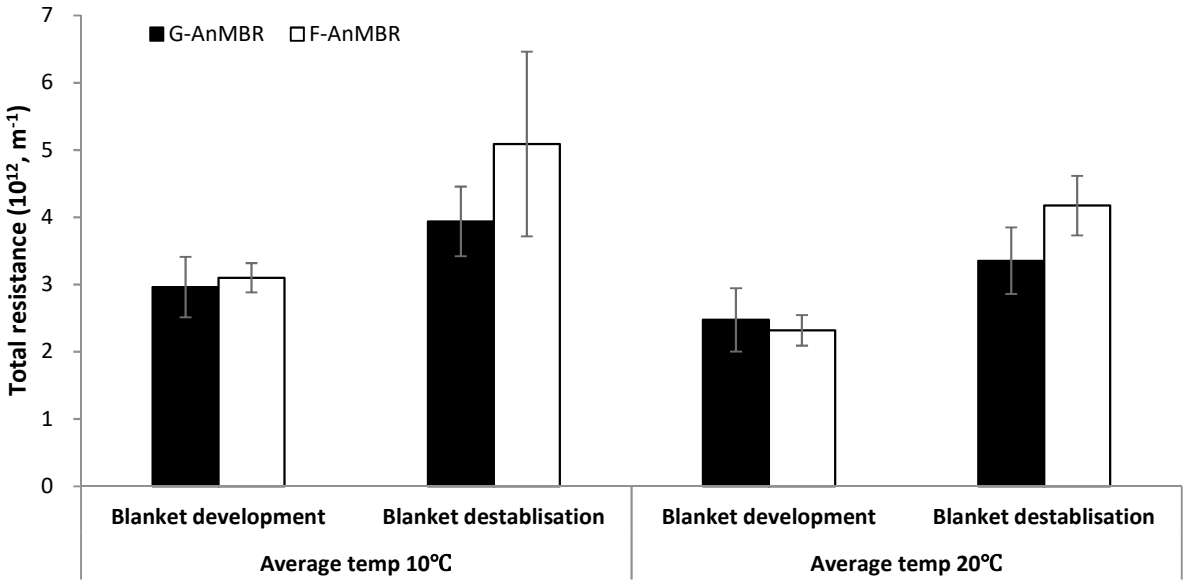

Figure 3. Total resistance in granular and flocculent AnMBR during sludge blanket development and blanket destabilisation at an average temperature of 10 and 20°C. Filtration/relaxation, 10min on/1min off, $J_{20\ net}$, 7.5 L m^{-2} h^{-1}; gas sparging, 10s on/10s off, SGD_m, 1.12 m^3 m^{-2} h^{-1}.

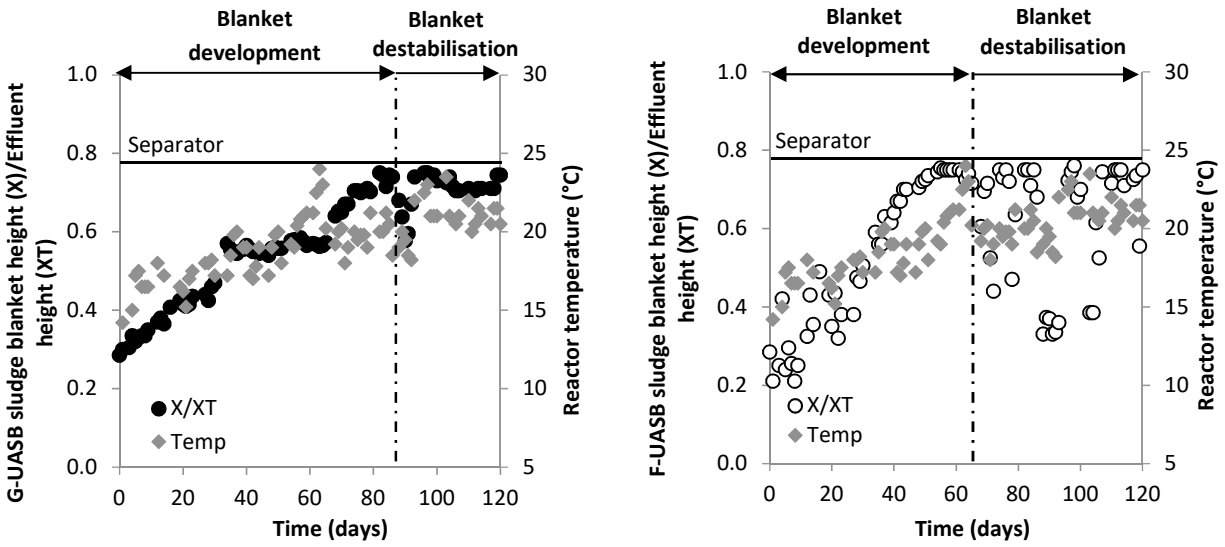

Figure 4. Temporal variation of UASB sludge blanket height (X)/Effluent height (XT) ratio and reactor temperature in G-UASB and F-UASB configured AnMBR. Sludge blanket development (0-86 d for G-UASB, 0-65 d for F-UASB); sludge blanket destabilisation (87-120 d for G-UASB, 66-120 d for F-UASB).

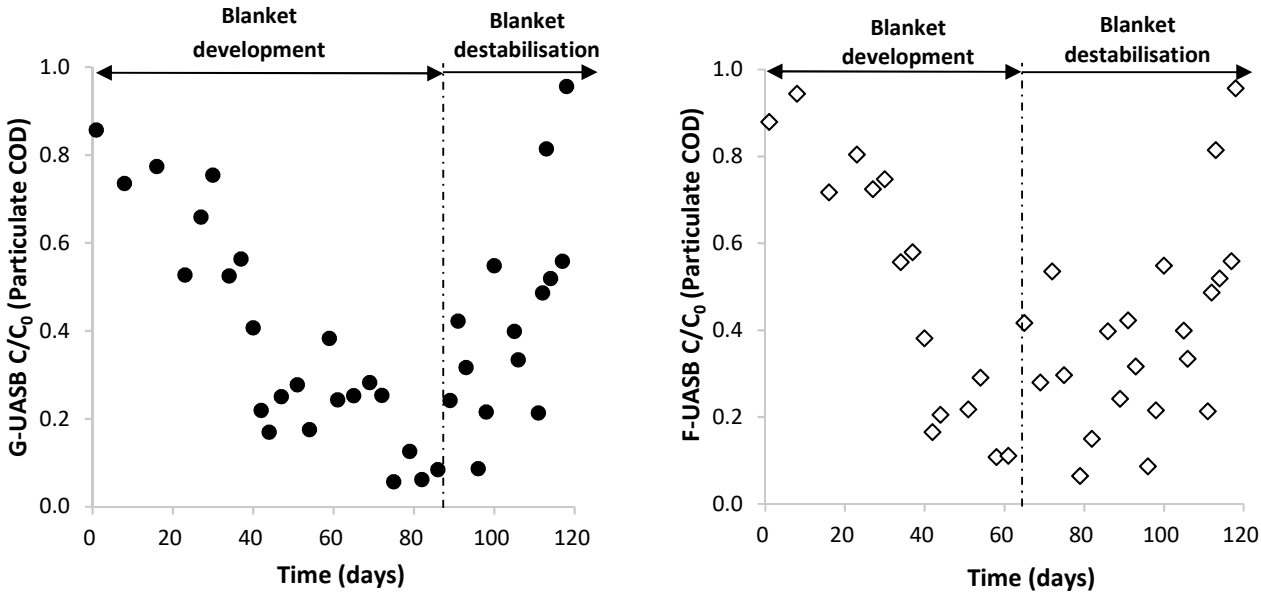

Figure 5. Impact of sludge blanket on particulate COD separation in the UASB reactors of granular and flocculent UASB configured AnMBRs (average temperature of 19.5±2.1 °C, COD_t=244±92 mg L^{-1}, pCOD=194±76 mg L^{-1}, $pCOD/COD_t$=0.80).

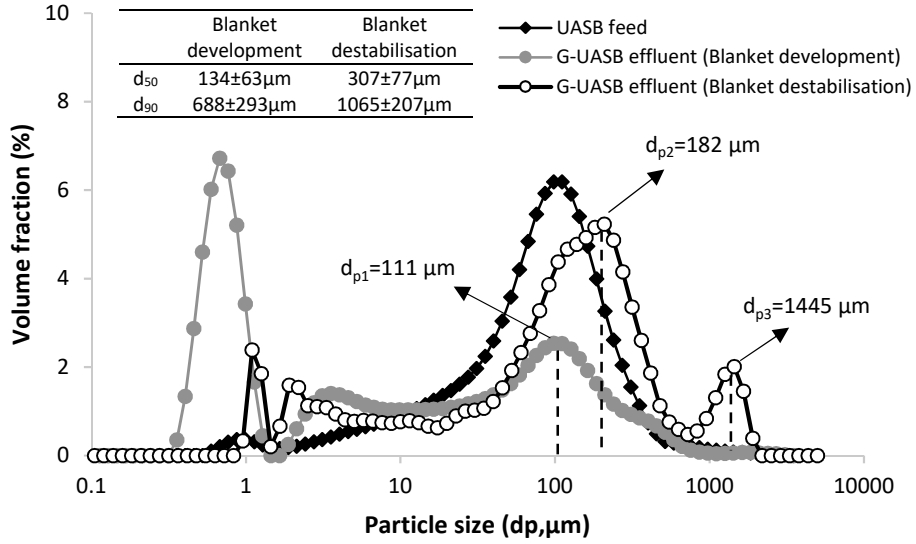

(a)

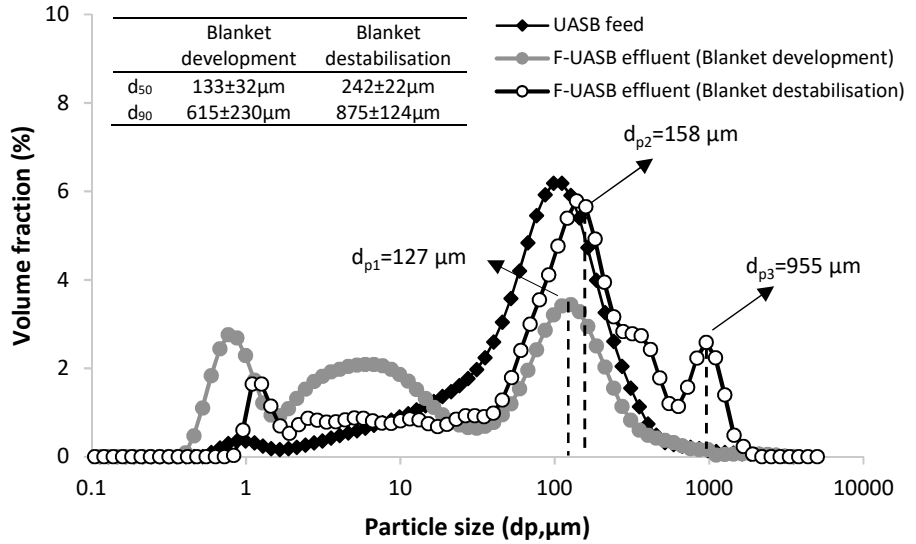

(b)

Figure 6. Particle size distribution of UASB feedwater, (a) G-UASB effluent and (b) F-UASB effluent before and after solids breakthrough in G-UASB and F-UASB configured AnMBRs.

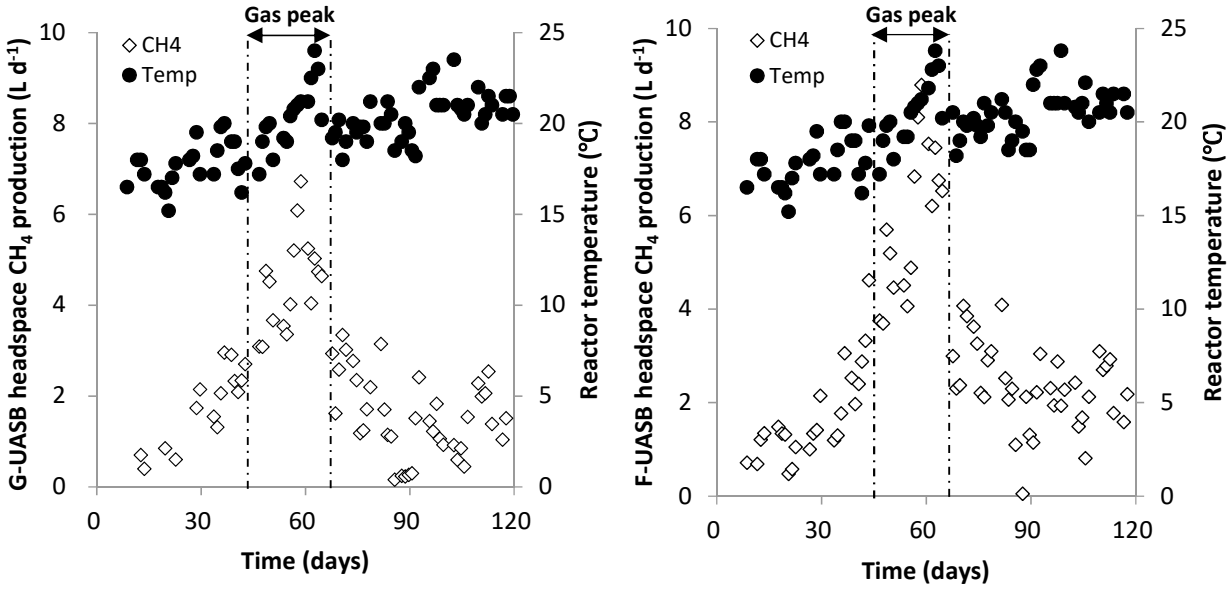

Figure 7. Headspace CH_4 production and reactor temperatures in G-UASB and F-UASB configured AnMBRs.

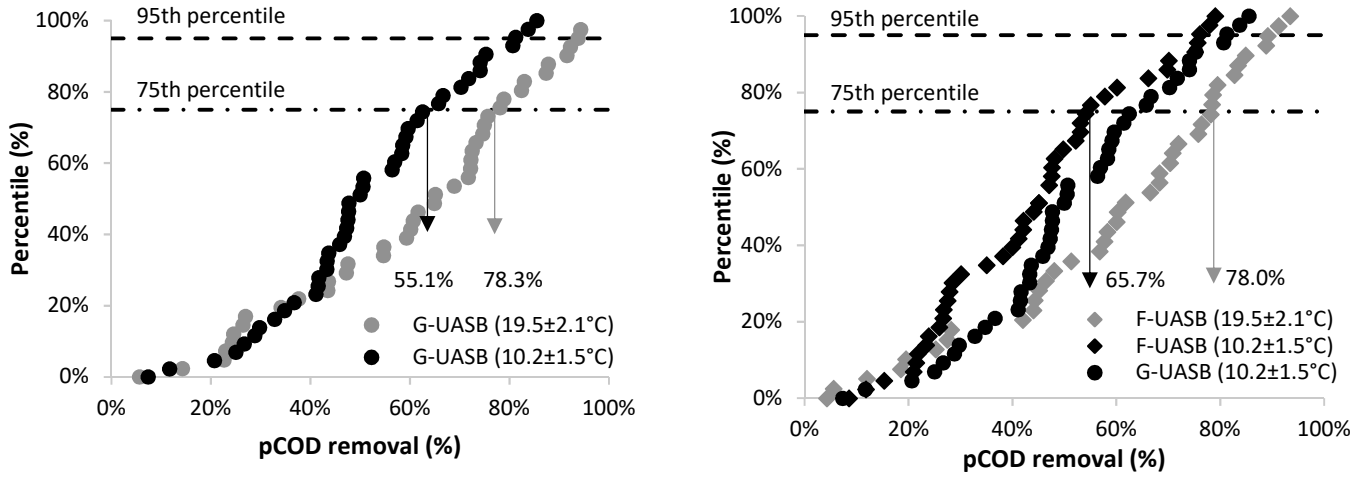

Figure 8. Impact of temperature on sludge blanket stability and particulate COD separation in G-UASB and F-UASB of UASB configured AnMBRs. 75th and 95th percentiles represent the frequency at which COD removal can be achieved during the temperature period stated.

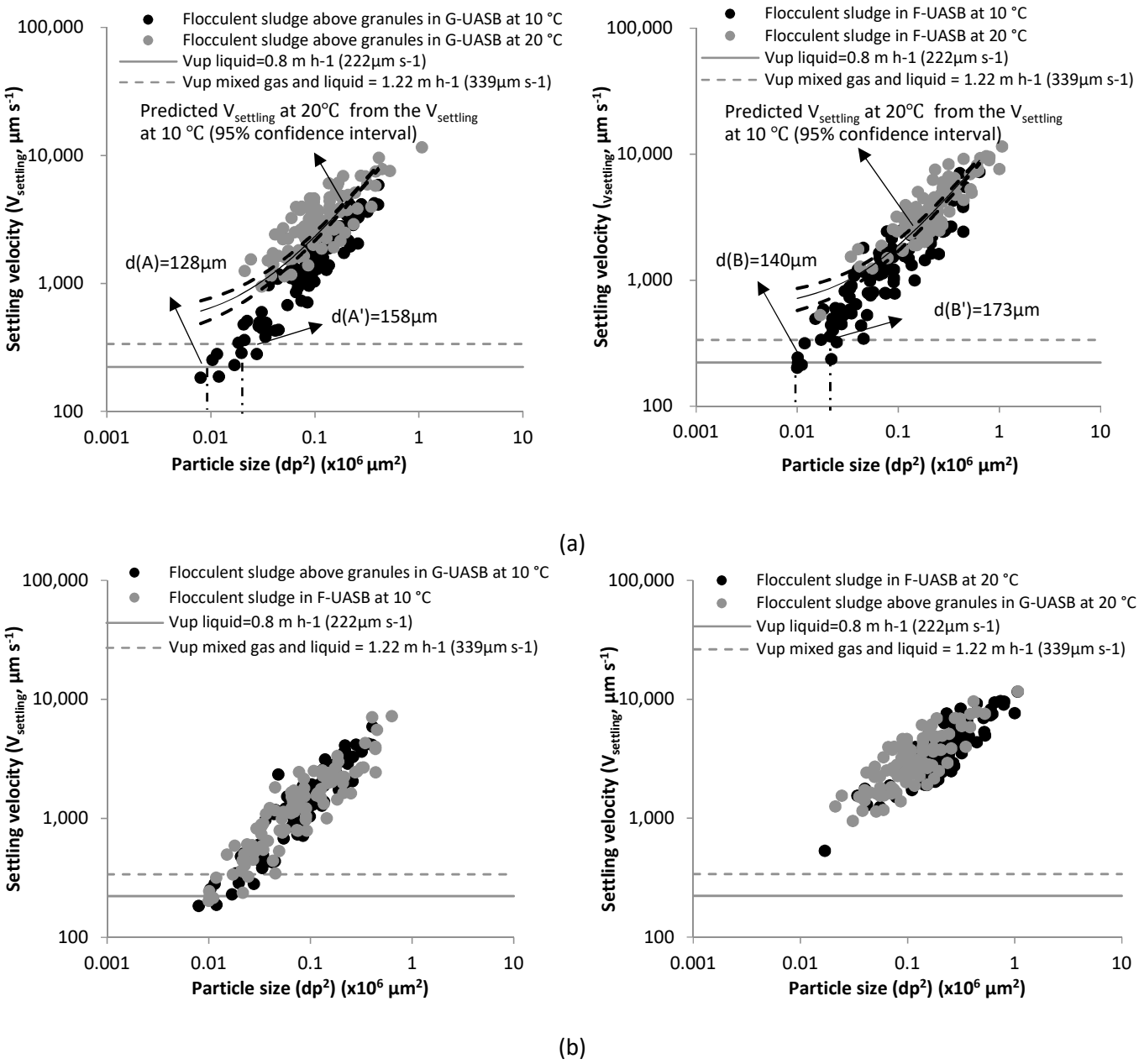

Figure 9. Impact of temperature on particle settling velocity in G-UASB and F-UASB (the average temperature when sampling particles from G-UASB and F-UASB reactors was 19.6±0.5 °C). (a) Impact of temperature on particle settling for flocculent sludge above granules in G-UASB and flocculent sludge in F-UASB at 10 and 20 °C. Black line represent linear trend line of predicted settling velocity at 20 °C calculated from the particle settling velocity at 10 °C. Dashed black lines represent confidence interval range (95 %). (b) Comparison of particle settling velocity between flocculent sludge above granules in G-UASB and flocculent sludge in F-UASB at 10 and 20 °C.

Table 1. Operational conditions of granular and flocculent UASB configured AnMBR

	Time period	**Average temp**
	days	°C
Phase I	120	19.5±2.1
Phase II	60	10.2±1.5

Table 2. Bulk sludge characteristics in the membrane tank of granular and flocculent AnMBR during sludge blanket development and blanket destabilisation at an average temperature of 10 and 20°C.

		Average temp 10°C				**Average temp 20°C**			
		Blanket development		**Blanket destabilisation**		**Blanket development**		**Blanket destabilisation**	
		G-AnMBR	F-AnMBR	G-AnMBR	F-AnMBR	G-AnMBR	F-AnMBR	G-AnMBR	F-AnMBR
MLSS	mg L^{-1}	280±35	288±59	498±77$^{\#}$	598±74$^{*,\#}$	207±20	202±38	294±30$^{\#}$	534±20$^{*,\#}$
CODt	mg L^{-1}	556±23	475±130	885±187$^{\#}$	1062±64$^{*,\#}$	331±15	313±81	560±35$^{\#}$	736±480$^{*,\#}$
pCOD	mg L^{-1}	390±13	348±94	697±113$^{\#}$	812±73$^{*,\#}$	250±28	218±68	460±32$^{\#}$	523±357$^{*,\#}$
SMP_{COD}[a]	mg L^{-1}	167±12	130±28	188±20$^{\#}$	250±42$^{*,\#}$	81±18	95±19	100±17$^{\#}$	209±124$^{*,\#}$

a. sCOD is equivalent to SMP_{COD}, samples were filtered through 1.2 µm filter paper.

*Statistical difference ($p<0.05$) between G-AnMBR and F-AnMBR during blanket development at average temperature of 10°C, G-AnMBR and F-AnMBR during blanket destabilisation period at average temperature of 10°C, G-AnMBR and F-AnMBR during blanket development at average temperature of 20°C, G-AnMBR and F-AnMBR during blanket destabilisation at average temperature of 20°C.

Statistical difference ($p<0.05$) between during sludge blanket development and blanket destabilisation period in G-AnMBR at an average temperature of 10°C, during sludge blanket development and blanket destabilisation period in F-AnMBR at an average temperature of 10°C, during sludge blanket development and blanket destabilisation period in G-AnMBR at an average temperature of 20°C, during sludge blanket development and blanket destabilisation period in F-AnMBR at an average temperature of 20°C.

Table 3. Impact of temperature on G-UASB and F-UASB treatment performance including sludge blanket development and blanket destabilisation period.

			G-UASB		F-UASB	
			10.2±1.5 °C	19.5±2.1 °C	10.2±1.5 °C	19.5±2.1 °C
UASB Effluent	SS	mg L^{-1}	69±11[#]	45±14	75±9[#,*]	54±14*
	COD_t	mg L^{-1}	129±19[#]	113±36	140±25[#,*]	122±35
	pCOD	mg L^{-1}	66±20[#]	57±30	80±17[#,*]	67±32
	sCOD	mg L^{-1}	64±13[#]	55±12	60±13[#]	54±14
	BOD_5	mg L^{-1}	84±8[#]	61±15	88±10[#]	61±15
Removal efficiency	SS	%	42±13[#]	64±12	36±14[#,*]	56±14*
	COD	%	41±14[#]	51±18	36±16[#,*]	45±22
	pCOD	%	52±18[#]	60±24	43±19[#,*]	55±25
	sCOD	%	18±12[#]	38±16	24±14[#]	39±15
	BOD_5	%	26±17[#]	46±14	19±11[#]	45±16
CH_4 production	Headspace + dissolved[a]	STP L d^{-1}	2.9±1.2[#]	6.7±1.7	6.6±0.8[#,*]	7.0±1.3*

STP: standard temperature and pressure

a. Dissolved CH4 estimated from Henry's law

*Statistical difference ($p<0.05$) between G-UASB and F-UASB at 20 °C, G-UASB and F-UASB at 10 °C

[#] Statistical difference ($p<0.05$) between G-UASB at 20 °C and G-UASB at 10 °C, F-UASB at 20 °C and F-UASB at 10 °C